

# Mechanistic Rationale for Ketene Formation during Dabbing and Vaping

Kaelas R. Munger, Killian M. Anreise, Robert P. Jensen, David H. Peyton, and Robert M. Strongin\*



Cite This: *JACS Au* 2024, 4, 2403–2410



Read Online

ACCESS |

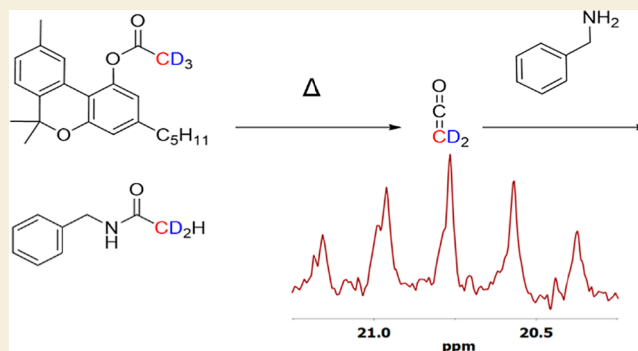
Metrics & More

Article Recommendations

Supporting Information

**ABSTRACT:** Ketene is one of the most toxic vaping emissions identified to date. However, its high reactivity renders it relatively challenging to identify. In addition, certain theoretical studies have shown that realistic vaping temperature settings may be too low to produce ketene. Each of these issues is addressed herein. First, an isotopically labeled acetate precursor is used for the identification of ketene with enhanced rigor in vaped aerosols. Second, discrepancies between theoretical and experimental findings are explained by accounting for the effects of aerobic (experimental) versus anaerobic (simulated and theoretical) pyrolysis conditions. This finding is also relevant to explaining the relatively low-temperature production of aerosol toxicants beyond ketene. Moreover, the study presented herein shows that ketene formation during vaping is not limited to molecules possessing a phenyl acetate substructure. This means that ketene emission during vaping, including from popular flavorants such as ethyl acetate, may be more prevalent than is currently known.

**KEYWORDS:** *vaping and dabbing, acetates, isotopic labeling, ketene*



## 1. INTRODUCTION

Ketenes comprise a unique class of cumulene molecules with the general formula  $RR'C=O$ . Initially described by Wedekind as a reactive intermediate in 1901,<sup>1</sup> Staudinger reported the first synthesis and characterization of a ketene molecule, diphenyl ketene ( $R=R'=Ph$ ), in 1905.<sup>2</sup> Since that time, despite their relative instability, ketenes have served as valuable reagents and intermediates in organic synthesis.<sup>3,4</sup> Currently, however, the smallest homologue ( $R=R'=H$ , ketene, ethenone) of the series is receiving attention as a potentially significant public health hazard,<sup>5</sup> since it has been identified in aerosols generated by commercial vaping products.<sup>6,7</sup>

The chemical and toxicological properties of ketene mirror those of phosgene ( $Cl_2C=O$ ), a WW-I chemical warfare agent, as a reactive acylating agent and respiratory poison.<sup>8</sup> There is a lack of human toxicity data for ketene exposure. The available animal data was obtained mainly prior to 1950. Exposure to animals causes alveolar damage and a delayed onset of pulmonary toxicity leading to death by pulmonary edema.<sup>8</sup> Similar to phosgene, the delayed effects result from the nonenzymatic acylation of lung proteins, as opposed to direct irritation. The Acute Exposure Guideline Levels (AEGL)-3 (life-threatening levels) for ketene are 0.24 ppm for 10 min and 0.088 ppm for 8 h.<sup>8</sup>

Vitamin E acetate (VEA) has been linked to the 2019–2020 e-cigarette or vaping product use–associated lung injury

(EVALI) epidemic, in large part due to VEA's prevalence in patient samples.<sup>9</sup> In 2020, Wu and O'Shea reported the formation of ketene when heating and vaping VEA,<sup>6</sup> indicating an additional possible link between ketene and EVALI. There is general agreement that EVALI is caused by chemical toxicant inhalation.<sup>10</sup> However, to date, neither ketene, VEA, nor any other specific chemical has been conclusively proven to be the causative agent of EVALI. Moreover, although there has been a significant decline since 2020, cases continue to be observed throughout the US.<sup>10</sup>

Regardless of whether VEA-derived ketene is a primary cause of EVALI, any source of exposure to ketene may put one at risk for a significant lung injury. Recently, we reported that four acetylated cannabinoids [acetylated  $\Delta^8$ - and  $\Delta^9$ -THC (tetrahydrocannabinol), CBN (cannabinol), and CBD (cannabidiol); **Figure 1**] produce ketene emissions under real-world vaping conditions from either a vape pen or dab platform, including at levels in range of National Institute for Occupational Safety and Health (NIOSH) thresholds.<sup>7</sup> Interestingly, aerosolized THC products had been reported

Received: May 14, 2024

Revised: May 31, 2024

Accepted: June 3, 2024

Published: June 12, 2024



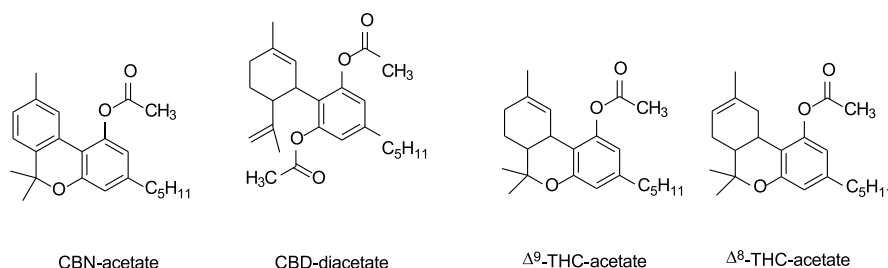
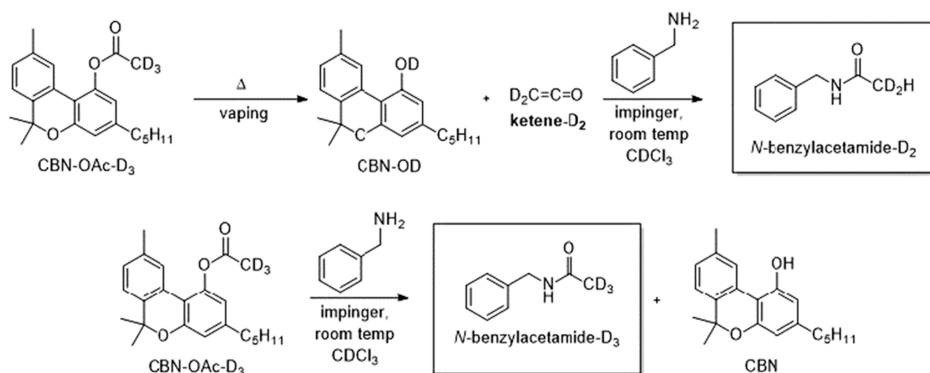


**Figure 1.** Cannabinoid acetates were previously shown to produce ketene emissions under vaping conditions. The study described herein focuses on CBN-acetate because it produces the relatively cleanest aerosol analytical data due to the added stability of its second aryl ring.

**Scheme 1. Top: Ketene Possesses a Methylene Carbon; Its Formation from a Trideuterated Acetate Will Therefore Result in *N*-Benzylacetamide- $D_2$ ; Bottom: Alternatively, *N*-Benzylacetamide- $D_3$  Will Form if a Different (e.g., Addition–Elimination) Mechanism Not Involving a Ketene Intermediate Is Relevant<sup>4</sup>**



<sup>4</sup>The addition–elimination transformation is a common method of amide formation. It is a potentially competing mechanism for other compounds (e.g., even the acetate precursors to ketene) besides ketene to form *N*-benzylamide. Control experiments (ref 7) showed that the reaction of acetates directly with benzylamine was too slow in the impinger to have occurred on the time-scale of our experiments and subsequent analyses. In the current paper, we have obtained additional rigorous evidence to distinguish between the addition–elimination mechanism and the ketene acetylation mechanism via the use of deuterium labeling.

to cause acute respiratory syndromes prior to the EVALI outbreak.<sup>11</sup>

The strong experimental evidence of ketene emissions arising from vaping cannabinoid acetates or VEA raises two issues. First, since ketene is too reactive and short-lived to be characterized as an intact molecule under common laboratory conditions, vaping studies to date have employed the well-known method of trapping ketene with a nucleophile (i.e., benzylamine) for characterization as the corresponding *N*-benzylacetamide. Since amines are relatively nonselective reagents, their use for ketene trapping and determination should ideally be limited to relatively well-defined systems that do not contain molecules that can react to form the same *N*-benzylacetamide product as ketene. However, manufacturers are not required to disclose most vaping product ingredients, and moreover, heating and vaping produce aerosols containing complex chemical mixtures.

To address this issue, herein, we describe the use of isotopically labeled CBN-acetate to rigorously identify ketene formation during vaping. All experiments were performed by using a commercially available device set at temperature settings consistent with normal user practices. The main hypothesis addressed via isotopic labeling is illustrated in Scheme 1: (Top) A characteristic dideuterated *N*-benzylacetamide product (*N*-benzylacetamide- $D_2$ ) would result if a ketene intermediate is formed from the trideuterated acetate methyl (i.e., CBN-OAc- $D_3$ ). (Bottom) Conversely, if ketene is not formed as a reaction intermediate, an alternative addition–

elimination or related reaction would result in trideuterated *N*-benzylacetamide (*N*-benzylacetamide- $D_3$ ).

The second issue centers on concerns that real-world vaping power settings do not provide enough energy to produce ketene. Recent theoretical studies show that unrealistically high vaping temperatures, in excess of at least 700 °C, are required for any significant levels of ketene to form from VEA or other acetates.<sup>5,12,13</sup> To address this issue, some have proposed that ineffective wicking (resulting in dry, overheated vaporizer coils, colloquially termed “dry puff”) or catalysis are potential causes of ketene production at relatively low power settings.<sup>12</sup> Alternatively, herein, we hypothesize that ketene formation at real-world vaping temperatures can be explained if one accounts for the impact of oxygen. This hypothesis is based on prior studies reported by our group in 2017,<sup>14</sup> as well as in subsequent reports by us<sup>15</sup> and by others.<sup>16,17</sup>

## 2. RESULTS

### 2.1. Synthesis and Mass Spectroscopic Analysis of CBN-OAc- $D_3$

Since a large portion of the volatile thermal reaction products of  $\Delta^8$  and  $\Delta^9$  THC formed under vaping conditions derive from their cyclohexene ring,<sup>18–20</sup> we focused current experiments on CBN-acetate. CBN-acetate contains a second aryl ring rather than a cyclohexene ring (Figure 1, see CBN-OAc- $D_3$ ) that renders it relatively stable, thereby reducing the analytical complexity of its corresponding aerosol samples. In addition,

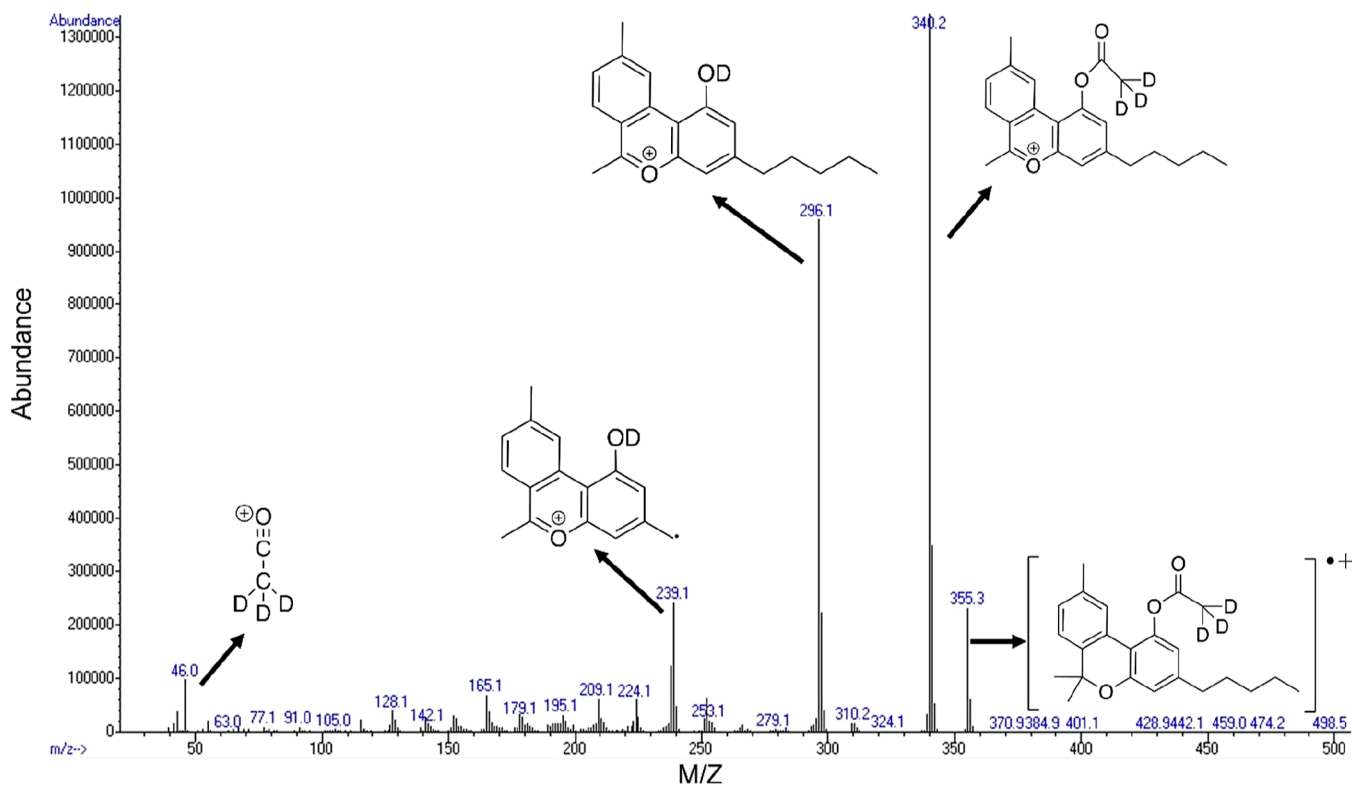


**Figure 2.** GC-EIMS (positive mode) of CBN-OAc-D<sub>3</sub> showing fragmentation involving the loss of ketene-D<sub>2</sub> (44 amu) from the base peak. The analogous spectrum for unlabeled CBN-OAc is shown in the [Supporting Information](#) and exhibits a loss of 42 amu and is consistent with the data shown in ref 5. The data for the trideuterated CBN-OAc show the expected *m/z* peak at 340 and a fragment *m/z* 296. The loss of 44 amu (vs 42 in the unlabeled version) corresponds to ketene via the loss of one deuterium, consistent with the top mechanism in [Scheme 1](#). In addition, these results are consistent with those reported in ref 5.

CBN and CBN-OAc are crystalline and thus easier to purify and handle compared with THC or CBD and their acetate derivatives.

CBN-OAc-D<sub>3</sub> was obtained in 85% yield by heating CBN and acetic anhydride-D<sub>6</sub> under neat conditions at reflux for 2 h. Previously, Nishida et al. synthesized trideuterated phenyl acetate to obtain evidence for the thermolytic mechanism of ketene formation.<sup>21</sup>

They determined that a four-membered ring transition state involving transfer of a hydrogen atom from the acetate methyl to the phenolic ester oxygen led to ketene. Consistent with this mechanism, we tentatively assigned the CBN-OD byproduct from deuterated ketene production shown in [Scheme 1](#) and [Figure 2](#) with a deuterated phenolic oxygen.

[Figure 2](#) shows the EIMS fragmentation pattern of CBN-OAc-D<sub>3</sub>. The corresponding data for CBN-OAc are displayed for comparison in [Figure S2](#). Loss of a geminal methyl from the structure corresponding to the molecular ion peak affords a base peak at 340 *m/z*. Loss of dideuterated ketene (44 amu) afforded the peak corresponding to CBN-OD (−CH<sub>3</sub>). In addition, it is also possible that ketene can be derived via deprotonation of the acylium ion fragment at 46 *m/z*. Another prominent peak appears at 239 *m/z*, arising from the loss of a four-carbon subunit from the cannabinoid pentyl side chain.

## 2.2. Aerosol Generation and Collection

In this and prior studies, we used a dabbing platform to heat and aerosolize cannabinoids.<sup>7,18–20</sup> Dabbing is a type of cannabis vaping that entails flash vaporization of manufactured cannabis products (e.g., high THC- or CBD-potency extracts) on a hot surface (colloquially referred to as a *nail*), with users

often inhaling close to an entire lung volume in one puff. A national web survey of cannabis consumers found that 60% of respondents dabbed at least once and that 38% endorsed its regular use.<sup>22</sup> Apart from embodying a popular means of cannabis vaping, using a dab platform has experimental advantages compared with vape pens. For example, the aerosols produced are not as prone to the influences of solvent, viscosity, metal filament catalysis, or variable wicking efficiency (e.g., dry coils) that can significantly impact vaping chemistry and aerosolization efficiency.<sup>19,20</sup>

The specific aerosolization and collection method used herein has been described by us previously, with minor changes (see [Supporting Information](#)).<sup>7</sup> Briefly, the cannabinoid sample (~100 mg) is flash vaporized on a quartz dab platform surface, and the generated aerosol is pulled via a smoking machine into an in-line impinger. The impinger contains an NMR solvent (CDCl<sub>3</sub>) and the trapping agent (benzylamine) at room temperature. Aliquots of the impinger solution containing the dissolved aerosol contents generated by a single puff are directly analyzed by NMR and GC–MS. The yield of ketene (as *N*-benzylamide equivalents) formed from 40 mg CBN-OAc under these conditions was 0.078 ± 0.016 mg (*n* = 4) at 378 °C, with 6–9% of the CBN-OAc converted to CBN.<sup>7</sup>

In the current study, we additionally studied the transformation of 40 mg of CBN-OAc to ketene at a lower temperature (250 °C) and obtained a 0.005 mg yield. Considering the 22%<sup>7</sup> trapping efficiency of ketene by benzylamine, the actual emission yield of ketene from just one puff is likely closer to ~5-fold higher (~0.025 mg) and

thus within an order of magnitude of the Acute Exposure Guideline Levels (AEGL)-3 (life-threatening levels, 10 min) for ketene (0.044 mg).<sup>8</sup> Moreover, there is no data reported for acute animal or human exposure to ketene.<sup>8</sup> Importantly, based on its analogous structure and properties compared to phosgene, there may likely be no “safe” levels of exposure to this highly toxic gas.

### 2.3. NMR and Mass Spectrometric Evidence for Ketene Formation

The production of *N*-benzylacetamide-D<sub>2</sub>, the “trapped” ketene equivalent product shown in Scheme 1, was unambiguously confirmed. The observed ESI-HRMS peak (Figure S4) at 150.0883 *m/z* is within 0.7 ppm of the calculated value (150.0882 *m/z*). Significantly, the proton-decoupled <sup>13</sup>C NMR spectrum, run at 100 MHz for 1024 scans and a D1 time of 4 s, shows a characteristic quintet splitting pattern centered at 20.8 ppm for CD<sub>2</sub>H, *J* = 20 Hz (Figure 3). See also Supporting Information for methodological details.

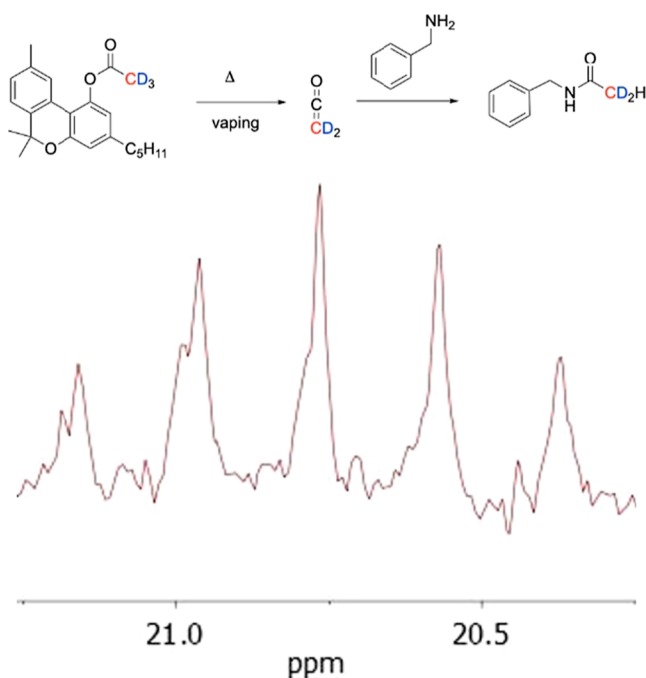


**Figure 3.** Expansion of the <sup>13</sup>C NMR spectrum (CDCl<sub>3</sub>) of the aerosol generated under flash vaporization conditions (378 °C) on a quartz surface showing the anticipated quintet splitting pattern (*J* = 20 Hz) corresponding to the dideuterated acetate methyl carbon of *N*-benzylamide-D<sub>2</sub>. See also Figures S6 and S7.

### 2.4. Control Experiments

Three additional experiments were conducted to provide additional evidence for ketene formation under real-world conditions. The first involved demonstrating that unreacted CBN-OAc is not a competing substrate in the impinger for benzylamine (see Scheme 1, bottom).

We stirred CBN-OAc for up to 8 h in a control impinger solution containing CDCl<sub>3</sub> and benzylamine. No *N*-benzylacetamide formation was observed in the <sup>1</sup>H NMR spectrum.

In contrast, in the vaping experiments, the <sup>1</sup>H NMR spectrum of the impinger solution showed the presence of *N*-benzylacetamide within minutes of aerosol generation and collection. Moreover, had CBN-OAc-D<sub>3</sub> (rather than ketene-D<sub>2</sub>) directly reacted with benzylamine, a septet arising from –

CD<sub>3</sub> splitting (from *N*-benzylacetamide-D<sub>3</sub>) would have been observed in the <sup>13</sup>C NMR, rather than the quintet shown in Figure 3.

The purity of CBN-OAc-D<sub>3</sub> was confirmed prior to the vaping experiments (Figure S3). Purification of CBN-OAc-D<sub>3</sub> was performed by dissolving the crude reaction mixture in an excess of hot ethanol, from which the desired product crystallizes upon cooling.

Acetic anhydride reacts rapidly and irreversibly with alcohols such as ethanol, especially at elevated temperatures; upon solvation, any residual acetic anhydride-D<sub>6</sub> forms trideuterated acetic acid (AcOH-D<sub>3</sub>) and trideuterated ethyl acetate (EtOAc-D<sub>3</sub>), which both join the mother liquor and wash cleanly away from the CBN-OAc crystals. However, if any residual acetic anhydride-D<sub>6</sub> remained in the sample and was responsible for the formation of *N*-benzylacetamide, the <sup>13</sup>C resonance from the resultant trideuterated acetate methyl carbon would appear as a septet rather than the observed quintet.

A second control study was performed to validate the feasibility of relatively lower vaping temperatures, leading to the formation of ketene. Each of the dab platform experiments described above was initially run at 378 °C, in keeping with our prior studies.<sup>7</sup> During the course of this study, we collaborated on a peer-reviewed systematic survey and analysis of user-preferred THC-acetate dabbing temperatures.<sup>23</sup> Temperatures ≥378 °C were preferred by 8% of respondents. For relevance to a wider range of users, we thus investigated and found readily detectable (<sup>1</sup>H NMR, Figure S1) levels of ketene as *N*-benzylacetamide equivalents when the aerosolization was performed at 250 °C, a temperature setting at or above which >70% of the survey respondents reported dabbing and 40% of respondents reported vaping.<sup>23</sup>

To investigate the potential role of oxygen in ketene formation, we dabbled ethyl acetate (EtOAc, Figure 4) and geranyl acetate (Figure S5) at 378 °C in a glovebag in ambient air (~21% O<sub>2</sub>) conditions and also under N<sub>2</sub> (<0.1% O<sub>2</sub>).

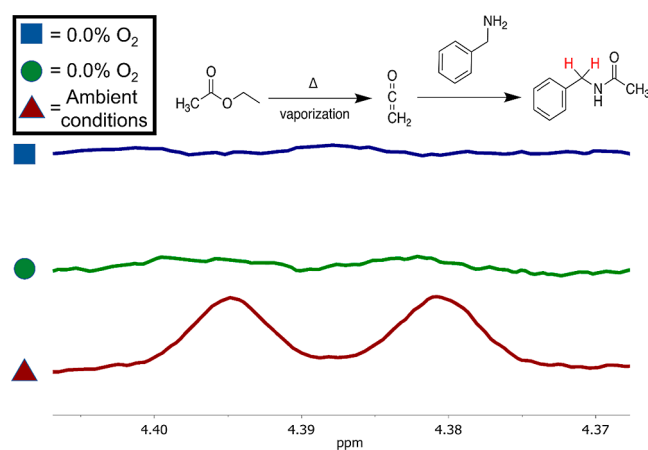


**Figure 4.** Expanded <sup>1</sup>H NMR spectra showing the methylene protons of *N*-benzylamide that was formed upon collection of the aerosol generated by ethyl acetate under ambient atmospheric conditions (red, bottom spectrum) along with two trials conducted in a 0.0% O<sub>2</sub> (<LOD of instrument) atmosphere, displayed in the green (middle) and blue (top) spectra. qNMR analysis of the samples was conducted and shows that ambient atmospheric conditions generated ten times the amount of ketene (trapped as *N*-benzylacetamide) when compared to the ketene generated under anaerobic conditions.



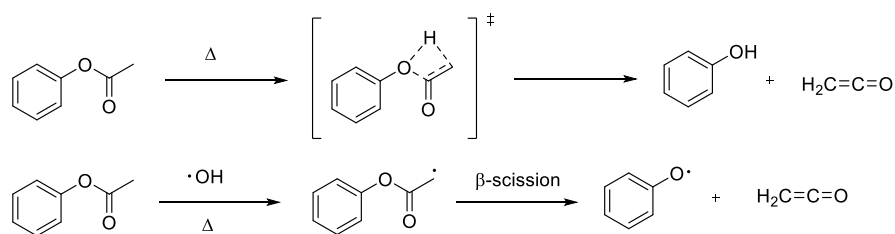


**Figure 5.** Two mechanisms for formation of ketene from phenyl acetate. Top: the published concerted four-membered ring transition state (ref 21). Bottom: mechanism involving oxygen-derived hydroxyl radicals analogous to that previously described for ketene formation from the combustion of small aliphatic acetates such as ethyl, methyl, and isopropyl acetate (refs 32 and 33).

EtOAc or geranyl acetate (500  $\mu\text{L}$ ) was used in these experiments since they are liquids and thus more amenable to glovebag conditions. The transformation of EtOAc to ketene had been simulated by others, with vaping temperatures  $>840\text{ }^\circ\text{C}$  needed to afford enough ketene to be introduced into a user's lungs.<sup>13</sup>

However, Figure 4 shows that, at  $378\text{ }^\circ\text{C}$ , *N*-benzylacetamide derived from dabbing EtOAc is  $\sim 10$ -fold higher under ambient aerobic (0.025 mg) versus reduced  $\text{O}_2$  conditions (0.0025 mg). Importantly, EtOAc is a prevalent flavorant molecule used in tobacco e-cigarettes. It was observed to be the fifth most frequently occurring flavor chemical in a study of 277 e-liquid products.<sup>24</sup> Geranyl acetate is a common terpene found in various cannabis concentrate blends and in e-liquids; terpenes are the second most abundant flavorant class in e-liquids.<sup>24</sup> Geranyl acetate (Figure S5) exhibited analogous behavior, with  $\sim 20$ -fold more ketene generated under ambient aerobic conditions.

### 3. DISCUSSION

The safety and regulation of vaping products are controversial issues, arguably among the most polarizing in the history of tobacco control.<sup>25,26</sup> Evaluation of tobacco as well as cannabis vaping products must include an understanding of their emissions, since significant chemical reactions occur upon both product storage and heating and vaping. Determining not only the identities of toxicant emissions but also their origins can support efforts toward improved product safety.

Ketene is one of the most toxic vaping emissions identified to date. To address exposure, it is necessary to identify ketene at its source; otherwise, its high reactivity renders its determination impractical in vivo or in vitro.<sup>27</sup> The use of an isotopically labeled acetate precursor (Scheme 1) enables rigorous ketene determination via  $^{13}\text{C}$  NMR splitting patterns and high-resolution mass spectrometry (Figure 3).

#### 3.1. Ketene Is Formed under Real-World Vaporization Temperatures

Ketene was detectable upon vaping CBN-acetate at vaping temperatures as low as, to date,  $250\text{ }^\circ\text{C}$  using a dab platform (Figure S1). This is consistent with our prior work, wherein ketene was detectable using a prefilled commercial vape cartridge and a low battery power setting.<sup>7</sup> However, according to theoretical simulations, ketene formation should not occur from vaping VEA,<sup>12</sup> cannabinoid,<sup>5</sup> or other acetates<sup>13</sup> at real-world vaping temperature settings.

To investigate catalysis and ketene formation, a preliminary analysis of used cannabinoid EVALI patient vape cartridge components by Wu and O'Shea uncovered features including nickel and chromium filaments within a charred, oil-soaked silica ceramic.<sup>6</sup> Catalysis could have potentially occurred via

the filaments, although charring is evidence of elevated temperatures. Benowitz et al.<sup>5</sup> later confirmed our finding of ketene formation from vaping cannabinoid acetates,<sup>7</sup> noting that catalytic sites in the devices can play a role. To the best of our knowledge, quartz (as used herein) has also not (to date) been identified as a heating component involved in catalysis during vaping. One of the reasons we used a quartz dabbing surface and not a vaporizer with metal heating coils is that we are able to eliminate metal coil catalytic<sup>28</sup> and solvent front (film boiling)<sup>29</sup> effects. There is another potential cause of ketene and other toxicant emissions at relatively low vaping power settings. We first reported the effect of aerobic conditions on vaping chemistry in 2017.<sup>14</sup>

The influence of aerobic conditions on the formation of toxic degradation products via hydrogen atom abstraction is consistent with the studies of Son<sup>30</sup> and Canchola<sup>31</sup> who showed that hydroxyl radicals are produced during vaping. Moreover, subsequent studies by other researchers confirmed that  $\text{O}_2$  is a major factor in promoting aerosol toxicant formation in the presence or absence of metal catalysts and at relatively mild vaping temperatures.<sup>16,17</sup>

The results shown in Figure 4 embody strong evidence that ketene emissions are  $\text{O}_2$ -dependent. Dabbing EtOAc as well as geranyl acetate showed clear reductions in ketene yields under anaerobic versus aerobic conditions. As noted above, theoretical studies have shown that ketene is not expected to form from VEA or EtOAc, for example, at vaping temperatures  $< 700\text{--}850\text{ }^\circ\text{C}$ , respectively. The simulated reaction pathways had activation energies of  $>50\text{ kcal/mol}$ , which is associated with temperatures much higher than normal vaping conditions. However, the simulations were carried out under anaerobic (pyrolysis) conditions, which therefore can account for the discrepancies between the theoretical and experimentally observed temperatures.

Figure 5 shows the mechanism of formation of ketene from phenyl acetate via the four-membered ring transition state proposed by Nishida et al. in 1974,<sup>21</sup> along with a proposed mechanism involving a hydroxyl radical described in prior published acetate combustion studies. The latter transformation involves proton abstraction by hydroxyl radical followed by  $\beta$ -scission to afford ketene.<sup>32,33</sup> Importantly, as noted above,  $\text{O}_2$ -derived hydroxyl radicals are prevalent during vaping.<sup>30</sup>

In using EtOAc and geranyl acetate to compare ketene production under anaerobic and aerobic environments, the results (Figure 4) showed that acetates, besides phenyl acetate-containing VEA and cannabinoids, can serve as ketene precursors. This is significant since ester flavorants are the most common class of tobacco e-cigarette flavorants. Exposure to ketene emissions may thus be more prevalent than currently

known. This finding suggests the need for further studies on vaping and ketene emissions as well as ketene toxicology.

## 4. CONCLUSIONS

Two main issues were addressed during the studies reported herein. First, rigorous evidence for ketene formation during vaping was obtained via the use of an isotopically labeled acetate precursor. Second, ketene formation was shown to be feasible at common vaping temperature settings. Moreover, under anaerobic conditions, ketene formation was inhibited, demonstrating that the role of oxygen and hydroxyl radicals should be taken into account when investigating the mechanism of ketene formation. In addition, we found that ketene formation was not limited to molecules containing a phenyl acetate substructure. These findings show that theoretical models based on anaerobic pyrolysis studies may provide an insufficient estimate of the thermal oxidation chemistry that is possible under real-world vaping and dabbing conditions. In addition, the work herein highlights the significant ongoing need for a greater understanding of the toxicology of vaping product ingredients as well as the chemical reactions occurring during vaping. Further investigations into the scope of ketene formation from additional ester-containing flavorant additives are ongoing in our laboratories and will be reported in due course.

## 5. METHODS

### 5.1. Materials

All NMR experiments described herein were performed on a Bruker AVANCE III 400 MHz NMR spectrometer. All  $^{13}\text{C}$  NMR experiments (100 MHz) were run with 1024 scans. HPLC-MS analysis was conducted on a ThermoFisher Scientific Q Exactive high-resolution time-of-flight mass spectrometer (HR-TOF-MS) using electrospray ionization. Gas chromatography mass spectrometry (GCMS) was performed on a capillary GC column mounted in an Agilent (Santa Clara, CA) 7890A GC interfaced to an Agilent 5975C MS and operated in electron impact ionization mode. Mass fragmentation patterns were compared to the NIST database to generate a percent match based on the observed fragmentation pattern. CBN was obtained from Florasience with 99% purity. All other chemicals were received from Sigma-Aldrich and used without purification.

### 5.2. Synthesis of CBN-OAc-D<sub>3</sub>

CBN (3.0 g) was heated at reflux with 1.5 mL of acetic anhydride-D<sub>6</sub> for 2 h at 200 °C. While the solution was still warm, 15 mL of 70 °C EtOH was added, and the mixture was cooled for 24 h. The CBN-OAc-D<sub>3</sub> crystallized and was filtered and dried under vacuum. A second volume equivalent of EtOH was added to the filtered crystals and heated at 70 °C until complete dissolution, at which time the solution was cooled for 24 h at room temperature, affording recrystallized CBN-OAc-D<sub>3</sub>. The crystals were filtered, dried under vacuum, and weighed (3.0 g, 88% yield, 99% purity by GC-MS). The  $^1\text{H}$  NMR spectrum was identical to that of CBN-OAc synthesized previously<sup>7</sup> (except for the deuterated acetate methyl proton peaks).

### 5.3. Aerosol Generation and Collection

An EKS REX-C100 temperature controller was used for heating 500 mg of acetate on the quartz nail during the dabbing experiments. The impinger solution proportions were adjusted slightly from the prior studies to improve the resolution of the *N*-benzylacetamide methylene peak and avoid overlap with the benzylamine peak.<sup>7</sup> The solution in the impinger consisted of 950  $\mu\text{L}$  of  $\text{CDCl}_3$  (950  $\mu\text{L}$ ) and benzylamine (50  $\mu\text{L}$ ). This ratio was found through the analysis of multiple samples to optimize the reaction of benzylamine and ketene. Once the impinger was prepared, the nail was heated to 378 °C (or

287 °C), within the range of temperatures at which cannabis consumers typically dab. All flow rate values and puff durations were the same as previously described by us.<sup>7</sup>

After aerosol generation and collection over ~10 min using a CSM-STEP smoking machine, the solution was removed from the impinger, transferred to an NMR tube, and immediately run on the Bruker AVANCE III 400 MHz NMR spectrometer. Additional trials were performed, and samples were run on a high-resolution quadrupole mass spectrometer for analysis. The samples were diluted with MeOH (1.5 mL) and analyzed via direct injection with a solvent mix of 50/50% MeOH/H<sub>2</sub>O and a 2 min total run time: HR ESI-TOF Mass (negative mode)  $m/z = 150.0883$  (calc for  $\text{C}_9\text{H}_9\text{D}_2\text{NO} = 150.0882$  [M]<sup>-</sup>) for *N*-benzylacetamide.

### 5.4. Anaerobic Dabbing Experimental Setup

A Cole-Palmer glovebag (37 in. × 37 in. × 25 in.) was used for all anaerobic experiments. The glovebag contained the electronic nail used in previous dabbing experiments, the dabbing glassware, and the compound of interest (for this experiment, ethyl acetate or geranyl acetate was used). Three different lines were connected and sealed to the glovebag. One end of the bag was connected to the fume hood air line as well as another connection to an ultrapure N<sub>2</sub> gas cylinder so switchover could occur without breaking the seal on the system. The other side of the glovebag was connected to the fume hood vacuum. Initial pressurization of the bag was achieved by closing the front zipper on the bag and taping the gas lines to ensure a proper seal. Air was allowed to flow into the bag at 2 PSI until the bag was inflated to a suitable working size. After a 5 min equilibration period, the e-nail was turned on and allowed to heat to 378 °C. Once the desired temperature had been reached by the quartz surface (e-nail), 500  $\mu\text{L}$  of ethyl acetate was administered onto the nail. The aerosol was pulled into an impinger containing the same solvent ratio as that described in the section above. After 5 min, the impinger was disconnected from the system, and the solvent was transferred to an NMR tube for analysis. After the initial samples were collected under normal atmospheric conditions, the air line was turned off, and the ultrapure nitrogen line was opened up and allowed to flow into the bag at 2 PSI while the residual air was pulled out via the fume hood vacuum at the same rate. The system was allowed to normalize to anaerobic conditions (0.0% O<sub>2</sub> as measured by the VmcoV 4 in 1 gas detector). Once optimal conditions were obtained, the vacuum was turned off, and the same dabbing experiment was again conducted under N<sub>2</sub>. Analysis of the impinger solvent system via NMR was again performed.

## ■ ASSOCIATED CONTENT

### Supporting Information

The Supporting Information is available free of charge at <https://pubs.acs.org/doi/10.1021/jacsau.4c00436>.

Additional NMR, MS, and GCMS data for reaction materials and products (PDF)

## ■ AUTHOR INFORMATION

### Corresponding Author

Robert M. Strongin — Department of Chemistry, Portland State University, Portland, Oregon 97217, United States; [orcid.org/0000-0003-3777-8492](https://orcid.org/0000-0003-3777-8492); Email: [strongin@pdx.edu](mailto:strongin@pdx.edu)

### Authors

Kaelas R. Munger — Department of Chemistry, Portland State University, Portland, Oregon 97217, United States  
Killian M. Anreise — Department of Chemistry, Portland State University, Portland, Oregon 97217, United States  
Robert P. Jensen — Florasience Inc., Milwaukie, Oregon 97222, United States

David H. Peyton – Department of Chemistry, Portland State University, Portland, Oregon 97217, United States;  
orcid.org/0000-0001-5828-055X

Complete contact information is available at:  
<https://pubs.acs.org/10.1021/jacsau.4c00436>

### Author Contributions

Credit: **Kaelas R Munger** conceptualization, data curation, formal analysis, investigation, methodology, validation, writing-original draft, writing-review & editing; **Killian M. Anreise** data curation, investigation; **Robert P. Jensen** conceptualization, formal analysis, methodology, writing-review & editing; **David H. Peyton** conceptualization, data curation, formal analysis, methodology, writing-review & editing; **Robert M. Strongin** conceptualization, data curation, formal analysis, funding acquisition, investigation, methodology, project administration, resources, supervision, validation, writing-original draft, writing-review & editing.

### Notes

The authors declare no competing financial interest.

### ACKNOWLEDGMENTS

We thank the NIH for partial support of this work via award 1R16DA061946 and the NIH and FDA for partial support of this work via award R01ES025257. The content is solely the responsibility of the author and does not necessarily represent the views of the NIH and FDA. We also thank Portland State University for partial support.

### REFERENCES

- (1) Wedekind, E. Ueber die Gewinnung von Säureanhydriden mit Hilfe von tertiären Aminien. *Ber. Dtsch. Chem. Ges.* **1901**, *34*, 2070–2077.
- (2) Staudinger, H. Ketene, eine neue Körperklasse. *Ber. Dtsch. Chem. Ges.* **1905**, *38*, 1735–1739.
- (3) Allen, A. D.; Tidwell, T. T. Ketenes and other cumulenes as reactive intermediates. *Chem. Rev.* **2013**, *113*, 7287–7342.
- (4) Allen, A. D.; Tidwell, T. T. New directions in ketene chemistry: The land of opportunity. *Eur. J. Org. Chem.* **2012**, *2012*, 1081–1096.
- (5) Benowitz, N. L.; Havel, C.; Jacob, P.; O'Shea, D. F.; Wu, D.; Fowles, J. Vaping THC-O acetate: potential for another EVALI epidemic. *J. Med. Toxicol.* **2023**, *19*, 37–39.
- (6) Wu, D.; O'Shea, D. F. Potential for release of pulmonary toxic ketene from vaping pyrolysis of vitamin E acetate. *Proc. Natl. Acad. Sci. U.S.A.* **2020**, *117*, 6349–6355.
- (7) Munger, K. R.; Jensen, R. P.; Strongin, R. M. Vaping cannabinoid acetates leads to ketene formation. *Chem. Res. Toxicol.* **2022**, *35*, 1202–1205.
- (8) National Research Council and Committee on Acute Exposure Guideline Levels, In *Seventeenth Interim Report of the Committee on Acute Exposure Guideline Levels*. National Academies Press, Washington, DC, USA, 2010.
- (9) Blount, B. C.; Karwowski, M. P.; Shields, P. G.; Morel-Espinoza, M.; Valentin-Blasini, L.; Gardener, M.; Braselton, M.; Brosius, C. R.; Caron, K. T.; Chambers, D.; Corstvet, J.; Cowan, E. Vitamin E Acetate in Bronchoalveolar-Lavage Fluid Associated with EVALI. *N. Engl. J. Med.* **2020**, *17*, 6438.
- (10) Rebuli, M. E.; Rose, J. J.; Noël, A.; Croft, D. P.; Benowitz, N. L.; Cohen, A. H.; Goniewicz, M. L.; Larsen, B. T.; Leigh, N.; McGraw, M. D.; Melzer, A. C.; Penn, A. L.; Rahman, I.; Upson, D.; Crotty Alexander, L. E.; Ewart, G.; Jaspers, I.; Jordt, S. E.; Kligerman, S.; Loughlin, C. E.; McConnell, R.; Neptune, E. R.; Nguyen, T. B.; Pinkerton, K. E.; Witek, T. J. The E-cigarette or Vaping Product Use-Associated Lung Injury Epidemic: Pathogenesis, Management, and Future Directions: An Official American Thoracic Society Workshop Report. *Ann. Am. Thorac. Soc.* **2023**, *20*, 1–17.
- (11) McGraw, M. D.; Houser, G. H.; Galambos, C.; Wartchow, E. P.; Stillwell, P. C.; Weinman, J. P. Marijuana medusa: the many pulmonary faces of marijuana inhalation in adolescent males. *Pediatr. Pulmonol.* **2018**, *53*, 1619–1626.
- (12) Narimani, M.; da Silva, G. Does 'Dry Hit' vaping of vitamin E acetate contribute to EVALI? Simulating toxic ketene formation during e-cigarette use. *PLoS One* **2020**, *15*, No. e0238140.
- (13) Narimani, M.; Adams, J.; da Silva, G. Toxic Chemical Formation during Vaping of Ethyl Ester Flavor Additives: A Chemical Kinetic Modeling Study. *Chem. Res. Toxicol.* **2022**, *35*, 522–528.
- (14) Jensen, R. P.; Strongin, R. M.; Peyton, D. H. Solvent chemistry in the electronic cigarette reaction vessel. *Sci. Rep.* **2017**, *7*, 42549.
- (15) Korzun, T.; Lazurko, M.; Munhenzva, I.; Barsanti, K. C.; Huang, Y.; Jensen, R. P.; Escobedo, J. O.; Luo, W.; Peyton, D. H.; Strongin, R. M. E-Cigarette airflow rate modulates toxicant profiles and can lead to concerning levels of solvent consumption. *ACS Omega* **2018**, *3*, 30–36.
- (16) Jaegers, N. R.; Hu, W.; Weber, T. J.; Hu, J. Z. Low-temperature (<200 °C) degradation of electronic nicotine delivery system liquids generates toxic aldehydes. *Sci. Rep.* **2021**, *11*, 7800.
- (17) Li, Y.; Dai, J.; Tran, L. N.; Pinkerton, K. E.; Spindel, E. R.; Nguyen, T. B. Vaping aerosols from vitamin E acetate and tetrahydrocannabinol oil: chemistry and composition. *Chem. Res. Toxicol.* **2022**, *35*, 1095–1109.
- (18) Meehan-Atrash, J.; Luo, W.; Strongin, R. M. Toxicant formation in dabbing: the terpene story. *ACS Omega* **2017**, *2*, 6112–6117.
- (19) Meehan-Atrash, J.; Luo, W.; McWhirter, K. J.; Strongin, R. M. Aerosol gas-phase components from cannabis e-cigarettes and dabbing: mechanistic insight and quantitative risk analysis. *ACS Omega* **2019**, *4*, 16111–16120.
- (20) Meehan-Atrash, J.; Luo, W.; McWhirter, K. J.; Dennis, D. G.; Sarlah, D.; Jensen, R. P.; Afreh, I.; Jiang, J.; Barsanti, K. C.; Ortiz, A.; Strongin, R. M. The influence of terpenes on the release of volatile organic compounds and active ingredients to cannabis vaping aerosols. *RSC Adv.* **2021**, *11*, 11714–11723.
- (21) Nishida, S.; Imai, T.; Tsuji, T. Vacuum thermolysis of aryl acetates. A mechanistic study. *Chem. Lett.* **1974**, *3*, 1303–1304.
- (22) Daniulaityte, R.; Zatreh, M. Y.; Lamy, F. R.; Nahhas, R. W.; Martins, S. S.; Sheth, A. R.; Carlson, R. G. A Twitter-based survey on marijuana concentrate use. *Drug Alcohol Depend.* **2018**, *187*, 155–159.
- (23) Bone, C. C.; Klein, C.; Munger, K.; Strongin, R. M.; Kruger, D. J.; Meacham, M. C.; Kruger, J. S. Reviewing the risk of ketene formation in dabbing and vaping tetrahydrocannabinol-o-acetate. *Cannabis Cannabinoid Res.* **2023**.
- (24) Omaiye, E. E.; McWhirter, K. J.; Luo, W.; Tierney, P. A.; Pankow, J. F.; Talbot, P. High concentrations of flavor chemicals are present in electronic cigarette refill fluids. *Sci. Rep.* **2019**, *9*, 2468.
- (25) Wagener, T. L.; Meier, E.; Tackett, A. P.; Matheny, J. D.; Pechasek, T. F. A proposed collaboration against big tobacco: common ground between the vaping and public health community in the United States. *Nicotine Tob. Res.* **2016**, *18*, 730.
- (26) Carroll, D. M.; Denlinger-Apte, R. L.; Dermody, S. S.; King, J. L.; Mercincavage, M.; Pacek, L. R.; Smith, T. T.; Tripp, H. L.; White, C. M. Polarization within the field of tobacco and nicotine science and its potential impact on trainees. *Nicotine Tob. Res.* **2021**, *23*, 36–39.
- (27) Strongin, R. M. Toxic ketene gas forms on vaping vitamin E acetate prompting interest in its possible role in the EVALI outbreak. *Proc. Natl. Acad. Sci. U.S.A.* **2020**, *117*, 7553–7554.
- (28) Saliba, N. A.; El Hellani, A.; Honein, E.; Salman, R.; Talih, S.; Zeaiter, J.; Shihadeh, A. Surface chemistry of electronic cigarette electrical heating coils: Effects of metal type on propylene glycol thermal decomposition. *J. Anal. Appl. Pyrolysis* **2018**, *134*, 520–525.
- (29) Talih, S.; Salman, R.; Karam, E.; El-Hourani, M.; El-Hage, R.; Karaoghlanian, N.; El-Hellani, A.; Saliba, N.; Shihadeh, A. Hot wires

and film boiling: Another look at carbonyl formation in electronic cigarettes. *Chem. Res. Toxicol.* **2020**, *33*, 2172–2180.

(30) Son, Y.; Mishin, V.; Laskin, J. D.; Mainelis, G.; Wackowski, O. A.; Delnevo, C.; Schwander, S.; Khlystov, A.; Samburova, V.; Meng, Q. Hydroxyl radicals in e-cigarette vapor and e-vapor oxidative potentials under different vaping patterns. *Chem. Res. Toxicol.* **2019**, *32*, 1087–1095.

(31) Canchola, A.; Langmo, S.; Meletz, R.; Lum, M.; Lin, Y.-H. External factors modulating vaping-induced thermal degradation of vitamin E acetate. *Chem. Res. Toxicol.* **2023**, *36*, 83.

(32) Hoare, D.; Kamil, M. The combustion of ethyl acetate, methyl propionate, and i-propyl acetate. *Combust. Flame* **1970**, *15*, 61–70.

(33) Lam, K.-Y.; Davidson, D. F.; Hanson, R. K. High-Temperature measurements of the reactions of OH with small methyl esters: Methyl formate, methyl acetate, methyl propanoate, and methyl butanoate. *J. Phys. Chem. A* **2012**, *116*, 12229–12241.